

## 2009-2017 TRENDS OF **PM<sub>10</sub>** AIR QUALITY IN THE LEGENDARY RIOTINTO MINING DISTRICT OF SW SPAIN

Ana M. Sánchez de la Campa<sup>a,b\*</sup>, Daniel Sánchez-Rodas<sup>a,c</sup>, Gonzalo Márquez<sup>a,b</sup>, Emilio Romero<sup>b</sup>, Jesús D. de la Rosa<sup>a,d</sup>

<sup>a</sup> Center for Research in Sustainable Chemistry-CIQSO, Associate Unit CSIC-University of Huelva “Atmospheric Pollution”, Campus El Carmen s/n, 21071 Huelva, Spain

<sup>b</sup> Department of Mining, Mechanic, Energetic and Construction Engineering, ETSI, University of Huelva, 21071 Huelva, Spain

<sup>c</sup> Department of Chemistry, Faculty of Experimental Sciences, University of Huelva, 21071 Huelva, Spain

<sup>d</sup> Department of Department of Earth Sciences, Faculty of Experimental Sciences, University of Huelva, 21071 Huelva, Spain

### ABSTRACT

This study is the first to perform a chemical characterization and source contribution of particulate matter (PM<sub>10</sub>) occurring through the abandonment and reopening of a historical sulphide mine. This long-range analysis covers the period 2009–2017 in the Riotinto mining district (Iberian Pyrite Belt, Southwestern Spain), which is a mining district of world-class importance. This mine represents a susceptible anthropogenic emission source of toxic sulphide-associated elements in atmospheric particulate matter, which affects the air quality of the nearby areas. **A total of 567 samples of 24 h were collected from 2009 to 2017 in a rural station. The filters were analysed to determined Organic and elemental carbon, mayor and trace elements and water soluble compounds of PM<sub>10</sub>.**

The trends of PM<sub>10</sub> and geochemical characterisation were studied considering the following periods: mine abandonment (2009–2014) and the mine’s state during (2015–2016) and after (2017) implementation of new emission abatement technology at this mine. The results revealed relatively high concentrations of Cu, Zn, Pb, As, Sb, and Bi during 2015–2016. A reduction of 42–59% was observed after 2017 for the same elements in PM<sub>10</sub>. **Five sources were identified: regional, mining, aged sea salt, combustion + traffic and crustal, using Positive Matrix Factorization Model (PMF5).** The contribution of the mining factor was higher in the reopening period (4.2 µg m<sup>-3</sup>, 16%). These results have been confirmed by As speciation analysis, in which the low extraction percentage obtained is related to the origin of the metalloids associated with sulphide ores.

The reduction of emissions of atmospheric particulate matter in the mining processes is the main objective in the implementation of measures considering the technological progress for cleaner and sustainable mining. In the case of reopening of historical mines, with low ore grade and greater extraction of ore and rock, a major effort must be made in order to avoid a negative influence on the environment and human health.

Keywords: Air quality, PM<sub>10</sub>, arsenic, metals, mine

\*Corresponding author. E-mail address: [ana.sanchez@pi.uhu.es](mailto:ana.sanchez@pi.uhu.es) (A.M. Sánchez de la Campa)

## 1. Introduction

Mining activity and mainly open pit operations are considered the major sources of particulate emission to atmosphere (Nriagu and Pacyna, 1988), highlighting the operations of exploitation, transport, abandonment of mining and waste accident in coal, and metallic and no metallic ore (Table S1). Fugitive atmospheric particles matter (APM) exert a considerable influence on the concentration, toxicity (Bell et al., 2001; Plumlee and Morman, 2011) and the human health (Magas et al., 2007; Wild et al., 2009; WHO, 2013, Patra et al., 2016) (Table S1). These APM inside open mine regions show high levels of heavy metals and metalloids (Tsai and Cheng, 2004; Park and Kim, 2005) that can be transported to near areas, which affects the quality of air and human health. Recently, Csavina et al. (2012) considered the transport of heavy metals and metalloids by APM to be an important pathway for their redistribution in the environment. Hence, these pollutants can reach long distances before being finally deposited on the ground or inhaled (Rasmussen, 1998; Zota et al., 2009; Wai et al., 2016). However, studies on the dispersion of metals and metalloids in APM with mining activities are scarce, although the associated environmental and health risks are known (Brotons et al., 2010; Taylor et al., 2010; Csavina et al., 2011, Table S1).

Mining of Cu resources are taking high relevance in the current world due to the depletion of mineral resources and economic growth (Valenta et al., 2019). The reopening of metallic historical mining with low ore grade implies a greater extraction, movement and treatment of ore and rock (Lagos et al. 2018), and in consequence, a negative influence on the environment (Valenta et al. 2019).

~~In this work, we study a chemical characterization and source contribution of PM<sub>10</sub> occurring through the abandonment and reopening of the Riotinto historical sulphide mine, one of the more important open-pit Cu mines of Europe.~~

In the last decade, in the Iberian Pyrite Belt (SW Iberian Peninsula), a resurgence of metallic mining has occurred owing to increases in prices, especially for Cu, which favours the opening of new mines (e.g. Cobre las Cruces Mine) or reopening of other legendary ones such as the Riotinto mining district.

Relevant geochemical anomalies of APM related to mining processes in Las Cruces Mine, Seville province, has been interpreted in Sánchez de la Campa et al. (2015). They found higher concentrations of Cu and As than those in other urban and rural Spanish areas in which high concentrations of As, Se, Bi, Cd, and Pb have been described. However, arsenic speciation studies in PM<sub>10</sub> have established differences in its contribution, in which the average extraction efficiency of As in PM<sub>10</sub> samples depends on the origin of the APM.

In Riotinto, past mining, mineral processing, and smelting industries have generated great amounts of hazardous mining residues from its exploitation since pre-Roman times. Recently, the levels and chemical compositions of PM<sub>10</sub> (particles with aerodynamic diameter below or equal to 10 µm) and depositional particles in this area have been defined by Sánchez de la Campa et al. (2011) and Castillo et al. (2013), respectively.

In this work, we study a chemical characterization and source contribution of PM<sub>10</sub> occurring through the abandonment and reopening of the Riotinto historical mine, one of the more important open pit Cu mines of Europe. Our study focuses on the trend evolution of PM<sub>10</sub> and sulphide-associated elements concentrations regarding the monitoring of fugitive emission implemented at a Cu mine in the Riotinto mining district, SW Spain. The concentration of tracer elements such as As, Pb, and Zn occurring through mining activity has been determined in PM<sub>10</sub> during the period 2009–2017 in Nerva town, a rural zone located near the open pit. For trend analyses, three periods have been distinguished: mine abandonment (2009–2014) and during (2015–2016) and after (2017) the implementation of emission abatement technology at the Cu mine. The As speciation analysis as well as the extraction percentage obtained will permit knowledge the origin of As associate sulphide ores in PM<sub>10</sub>. The toxicity of As is dependent on its chemical form, oxidation state, and physical state of gas versus in solution (Pershagen et al., 1982; Viraraghavan et al., 1992). The reduction of emissions of APM in the mining processes is a main objective in the application of measures considering the technological progress for cleaner and sustainable mining.

## 2. Material and methods

### 2.1. The study area

The Riotinto mining district is one of the world's principal sulphide geochemical anomalies (Fig. 1) (Leistel et al., 1998). This region is of great historic interest and is considered as one of the largest volcanogenic massive sulphide outcrops worldwide, which has been exploited dating back to pre-Roman times (Davis et al., 2000). Its intense activity has been reflected in the notable environmental degradation of the area (Galán et al., 2003; Lottermoser, 2010). Mining operation in this district ceased in 2001 owing to low Cu prices. In 2015, a new mining project began with an initial production of 5 Mt per year in the pre-activity stage, evolving to 9.5 Mt per year in the full operational stage. During the mining inactivity period, the impacts of the fugitive particles and emissions in the air were minimal but were clearly identified (Sánchez de la Campa et al., 2011; Sánchez de la Campa et al., 2015).

The location of the sample monitoring station for PM<sub>10</sub> and a panoramic view of the waste mining area during the inactive and operational mining periods are shown in Fig. 1. The predominant wind directions for the study period 2009–2017 was NNE and WSW. These results are indicated in the wind rose diagram inset in Fig. 1.

## 2.2. Cu concentrate production at Atalaya mining project

In 2015, the historic mine of Riotinto has returned to activity through the Atalaya Mining Project in the Cerro Colorado area (Fig. 1). During mining activity, the extracted mineral is processed by crushing, grinding, and flotation to obtain Cu concentrate as the final product. During the primary crushing process, the ore is reduced to a size of 165 mm. This mineral is then stored in the 'coarse warehouse' and is later transported to the secondary and tertiary crushing circuit. During the first phase of this process, the material is screened to a size of approximately 16 mm and is later transferred to the 'fine warehouse'. Here, a primary mill reduces the mineral to its final size up to 1.5 mm. The mineral is later subjected to a series of cyclones that classifies the material by gravity in which the finer sizes overflow and pass to the flotation area, and the coarser sizes are moved to additional stages of grinding. From this process a fine dust of less than 160  $\mu\text{m}$  is obtained, which is mixed with water and pumped to the flotation area, where physical–chemical processes are used to recover the metallic content.

The Atalaya mining project reached a production capacity of 9.5 Mt of ore per year at the end of 2016, aided by an important process of modernisation of the metallurgical facilities, particularly in the construction of new grinding and flotation areas. The operation of the mining–metallurgical Atalaya project is estimated to be about 16 years.

The main control operations on air quality are related to the implementation of emission abatement technology of fugitive particles into the atmosphere. These consist of implementing irrigation, adaptation, and regeneration of tailings and planning of operations using atmospheric dispersion models to minimise the impact of APM on the surrounding population ([personal communication, Atalaya mining](#)).

## 2.3. Experimental methods

The period considered in this study was from 2009 to 2017.  $\text{PM}_{10}$  samples were collected by using a high-volume sampler (MCV CAV-PM1025 model,  $30 \text{ m}^3 \text{ h}^{-1}$ , [UNE-EN 12341:2015](#)) equipped with  $\text{PM}_{10}$  inlets installed on the roof of the Nerva town hall building, located about 1 km from the mine. Quartz filters (Munktell) were used for the collection of  $\text{PM}_{10}$ . Samples were collected for 24 h with a frequency of one filter every four days during the sampling period from 2009 to 2010. From 2011 to 2017, the frequency was one sample per week. [Five samples collected in the La Dehesa site \(see Fig. 1\) during intensive campaign of one month \(from 29 August to 29 September 2016\) has been included in this study in order to comparison to As speciation results with the obtains in Nerva station.](#)

The mass concentrations of  $\text{PM}_{10}$  were obtained by weighing the filters, using a Sartorius LA130 S-F balance with 0.1 mg sensitivity and using standard procedures of at 50% and 20 °C relative humidity and temperature, respectively. Afterwards, the half fraction of each of filter was digested in an acid solution with 2.5 ml  $\text{HNO}_3$ : 5 ml HF: 2.5 ml  $\text{HClO}_4$ , which was modified after the methodology reported by Querol et al. (2001). Analytical techniques such as Inductively coupled plasma optical emission spectrometry (ICP-OES; Jobin Yvon model ULTIMA2) was used for determination of major elements (Al,

Ca, K, Na, Mg, Fe, Ti, and Mn), and ICP-mass spectrometry (MS; Hewlett-Packard HP4500 and Agilent model 7700) was used to determination trace elements (Li, Be, Sc, V, Cr, Co, Ni, Cu, Zn, Ga, Ge, As, Se, Rb, Sr, Y, Zr, Nb, Mo, Cd, Cs, Ba, La, Ce, Pr, Nd, Sm, Eu, Gd, Tb, Dy, Ho, Er, Tm, Yb, Lu, Ta, W, Tl, Pb, Bi, Th, and U). The mean precision and the accuracy for most of the studied elements were in the range of 5–10% and were controlled by repeated analysis of NBS-1663a and NBS-1663b (fly ash) reference materials. The detection limit (DL) for most of elements in solution was 0.01 ppb.

The soluble fraction of a one-quarter part of each filter was extracted with Milli-Q grade deionised water at 60 °C. After leaching, the content of major anions ( $\text{SO}_4^{2-}$ ,  $\text{NO}_3^-$ , and  $\text{Cl}^-$ ) and  $\text{NH}_4^+$  in the leachates was determined by ion chromatography (Dionex DX-120; Methrom 883 Basic IC Plus) (Querol et al., 2002). Finally, during the period 2009–2013, a circular section punch 25 mm in diameter for each filter was employed to determine the total carbon ( $C_{\text{total}}$ ) content using an elemental analyser (LECO SC-144 DR equipment). From 2014 to 2017, a section of 1.5 cm<sup>2</sup> punch of each filter was analysed to determine the concentration of organic carbon (OC) and elemental carbon (EC) by a using thermal–optical transmission (TOT) technique employing an OC–EC analyser (Sunset Laboratory) with EUSAAR\_2 temperature protocol.

The detection limit for  $C_{\text{total}}$ , calculated on repetitive analysis of 10 blanks, was 0.4  $\mu\text{g cm}^{-2}$  per section of filter. The accuracy and precision of the TOT technique were below 5% and were determined after repeated analyses of standards of known concentration (sucrose 99.9% reagent grade; 42.1  $\mu\text{g cm}^{-2}$ ).

Speciation analysis of As (arsenite As(III) and arsenate As(V)) was performed by high performance liquid chromatography coupled with hydride generation and atomic fluorescence spectrometry (HPLC–HG–AFS) according to a methodology proposed for As speciation in APM (Oliveira et al., 2005; Sánchez-Rodas et al., 2007; Sánchez de la Campa et al., 2008). The detection limits obtained were 0.1 ng m<sup>-3</sup> for As(III) and 0.4 ng m<sup>-3</sup> for As(V).

To determine the temporal trend in the pollutant concentrations during the period 2009–2017, the Theil–Sen function included in the R programming language and its openair package for statistical analysis (Carslaw and Ropkins , 2012a; 2012b) was used considering the concentrations and chemical composition of PM<sub>10</sub> per day. A nonparametric Mann–Kendall test for the trend was applied by characterisation of the temporal trend analysis. The significance is represented by p. The symbols shown next to each trend estimated its statistical significance such that  $p < 0.001 = \text{***}$ ,  $p < 0.01 = \text{**}$ ,  $p < 0.05 = *$ , and  $p < 0.1 = +$ .

### 3. Results and discussion

The mean concentrations and chemical composition of PM<sub>10</sub> from 2009 to 2017 are shown in Table 1 considering the three periods established in this study: prior to abandonment and during and after the implementation of emission abatement technology. To describe and evaluate the statistically significant trends of all periods, the

long-term trend of PM<sub>10</sub> and its components were assessed by using the Theil–Sen approach (Table 1).

### 3.1. Mean PM<sub>10</sub> and chemical composition

The mean concentrations of PM<sub>10</sub> for the three study periods were highly similar, between 26 and 27 µg m<sup>-3</sup> (Table 1). These values are lower than the annual limit of 40 µg m<sup>-3</sup> established in the European Air Quality Directive (2008/50/EC) but are above the 19–21 µg m<sup>-3</sup> range reported for PM<sub>10</sub> at rural monitoring stations in Spain (Querol et al., 2004; Querol et al., 2008). However, no exceedance of the daily limit value, at 50 µg m<sup>-3</sup> (2008/50/EC) has been reported.

The concentrations of sulphide-associated elements such as Ti, Cu, Zn, As, Sn, Sb, Pb, and Bi as well as those of other elements and compounds are also summarised in Table 1 for the three periods established in this study. Overall, our results reveal that the highest mean concentrations for sulphide-associated elements were found during the initiation of mining activities, more specifically in 2016, at 62.4 ng m<sup>-3</sup>, 25.3 ng m<sup>-3</sup>, 49.1 ng m<sup>-3</sup>, 4.47 ng m<sup>-3</sup>, 0.78 ng m<sup>-3</sup>, 1.31 ng m<sup>-3</sup>, 11.5 ng m<sup>-3</sup>, 0.39 ng m<sup>-3</sup> for Ti, Cu, Zn, As, Sn, Sb, Pb, and Bi, respectively. It should be noted that the mean concentrations for this period do not exceed the 2008/50/EC target values of 6 ng m<sup>-3</sup> for As and 500 ng m<sup>-3</sup> for Pb. A concentration reduction of 13–57% was obtained in 2017 for these sulphide-associated elements after implementation of the current emission controls. The abatement techniques consist of irrigation, adaptation, and regeneration of tailings as well as planning of operations using atmospheric dispersion models. The concentration reductions, calculated from the data in Table 1, are Bi: 59%; Zn: 57%; As: 56%; Pb: 47%; Sb: 46%; and Cu: 42%. The lowest percentages were found for Sn and Ti, at 19% and 13%, respectively. Sánchez de la Campa et al. (2015) reported that the annual mean concentrations of these elements in Gerena, a town near the mining areas of the Iberian Pyrite Belt, were higher than in Nerva, highlighting the case of Cu, at 49.8 ng m<sup>-3</sup>. Similar concentrations were found for Ti: 43.9 ng m<sup>-3</sup>; Zn: 29.9 ng m<sup>-3</sup>; As: 1.52 ng m<sup>-3</sup>; Sn: 1.06 ng m<sup>-3</sup>; Sb: 0.61 ng m<sup>-3</sup>; Pb: 7.02 ng m<sup>-3</sup>; and Bi: 0.26 ng m<sup>-3</sup>.

The relatively high and similar concentrations found for C<sub>total</sub>, K, and Cl<sup>-</sup> during the three study periods are comparable to the values described by Sánchez de la Campa et al. (2011). This similar distribution can be associated to the influence of additional biomass burning sources.

### 3.2. Inter-annual variations

The analysed data were studied by using the Mann-Kendall test and the Theil–Sen algorithm. The trend estimate and statistical significance are shown in Table 1. The results show a representative rising trend in the annual average concentrations of sulphide-associated elements such as Ti, Mn, Cu, Zn, Mo, Ba, Zr, and Pb. In addition, a representative increasing trend in the annual mean concentrations of SiO<sub>2</sub> and Al<sub>2</sub>O<sub>3</sub> was observed. The rest of the elements and compounds did not present a clear trend estimate. High statistical significance ( $p < 0.001$ ) was found for K, Fe, PO<sub>4</sub><sup>3-</sup>, Li, Be, Sc,

As, Y, Zr, Sb, Hf, Tl, and Th, and lower statistical significance values ( $p < 0.01$  and  $p < 0.05$ ) were obtained for  $\text{SiO}_2$ ,  $\text{Al}_2\text{O}_3$ , Mn, Co, Cu, Mo, Cs, U, Mg,  $\text{NH}_4^+$ , Ti, Cr, Ga, Ge, Se, Rb, Nb, La, Ce, and Pb. The lowest significance ( $p < 0.1$ ) corresponds to Sr. No statistical significance was observed for the remaining elements and compounds.

Seasonal variation was observed for the concentration of some sulphide-associated elements in  $\text{PM}_{10}$ . A smooth trend with a 96% confidence interval was performed, as shown in Fig. 2. The maximum concentrations of Cu, As, Bi, Pb, and Sb were always found in summer during the 2015–2016 period. In addition, high concentrations of these elements were found in autumn during the same period. These maximum concentrations are related to the reopening of the Atalaya mine in 2015–2016, which is coincident with this same period. In winter, increases in the sulphide-associated elements were not observed owing to the high frequency of Atlantic mass and precipitation registered during this season of the year.

### 3.3. Source contribution of $\text{PM}_{10}$

Positive matrix factorisation was performed on the dataset recorded from 2009 to 2017 in Nerva. The results obtained during the three periods considered in this study were also included, with the following five factors identified (Fig. 3).

- F1 (regional) is characterised by  $\text{NH}_4^+$ ,  $\text{SO}_4^{2-}$ , and  $\text{NO}_3^-$ . V, Ni, and Zn have also been identified in this source. The ions are associated with secondary aerosols. The presence of Ni, V, and Zn was affected by industrial combustion of fossil fuel (Viana et al., 2008). The annual maximum contributions were  $4.7 \mu\text{g m}^{-3}$  in 2009 and 2010 and  $4.4 \mu\text{g m}^{-3}$  in 2016 (Fig. 4). A seasonal variation was observed, highlighting the maximum concentration of this source during summer (Fig. 3). The highest levels of solar radiation were relevant during this period. The F1 source accounted for 15% of the  $\text{PM}_{10}$  mass, at  $3.7 \mu\text{g m}^{-3}$ .
- F2 (mining) has a chemical profile similar to that of raw material extracted from Atalaya mine, which is defined mainly by Bi, Cu, As, Sb, Pb, and Zn. This chemical profile is similar to that described in the industrial estate located near the city of Huelva (Pb, As, Cu, Cd, Sn, Zn and  $\text{PO}_4^{3-}$ , Alastuey et al., 2006), as well as the Riotinto mine Sánchez de la Campa et al., 2011) and the Cobre las Cruces mine (Sánchez de la Campa et al., 2015). The contribution of the F2 source was less than  $1 \mu\text{g m}^{-3}$  between 2009 and 2014, which is related to inactivity of the mining–metallurgical operation of Atalaya mine. The maximum contribution, at  $4.2 \mu\text{g m}^{-3}$ , was observed in 2016 related to the start of the extraction activity followed by a decrease to  $2.6 \mu\text{g m}^{-3}$  in 2017 related to the implementation of emission abatement technology (Fig. 4). The F2 source accounted for 7% of the  $\text{PM}_{10}$  mass, at  $1.7 \mu\text{g m}^{-3}$ .
- F3 (aged sea salt) is characterised by elements related to the mixing of marine aerosols such as Na,  $\text{Cl}^-$ , and Mg with elements of ship emission affinity such as  $\text{NO}_3^-$  and  $\text{SO}_4^{2-}$  (Viana et al., 2014). The maximum contribution of F3 was  $5.4 \mu\text{g m}^{-3}$ .

$\text{m}^{-3}$  in 2013 and, and the value was constant at  $3.4\text{--}4.5 \mu\text{g m}^{-3}$  during the rest of the study period (Fig. 4). The minimum contribution of  $2.2 \mu\text{g m}^{-3}$  was obtained in 2011. The marine aerosol did not show a clear seasonal pattern (Fig. 3). This source accounted for 16% of the  $\text{PM}_{10}$  mass, at  $4.0 \mu\text{g m}^{-3}$ .

- F4 (combustion + traffic) contains K,  $\text{C}_{\text{total}}$ , and  $\text{NH}_4^+$  as well as  $\text{NO}_3^-$ , Cr, Zn, and Pb. Major elements and compounds such as  $\text{C}_{\text{total}}$ , K, and  $\text{NO}_3^-$  are associated with both sources, whereas the presence of trace metals such as Cr, Zn, and Pb are representative of traffic emissions. The temporal variation of this factor displayed high concentrations during winter (Fig. 3). It should be noted that in Nerva and its nearby areas, wood burning in fireplaces is the main biomass burning source. The annual distribution of this source was constant during the entire period at  $7.5\text{--}8.5 \mu\text{g m}^{-3}$ . However, a peak concentration of  $10.5 \mu\text{g m}^{-3}$  was characterised in 2011 (Fig. 4). The F4 source accounted for 32% of the  $\text{PM}_{10}$  mass, at  $8.1 \mu\text{g m}^{-3}$ .
- F5 (crustal) is constituted by elements related to the resuspension of crustal material and soil dust such as Al, Ca, K, Mg, Fe, Rb, Sr, Li, and La. The highest contributions of this source were recorded in summer, a period characterised by the minimum rainfall levels along the year and by the increase in the frequency of Saharan dust outbreaks (Rodríguez et al., 2001) (Fig. 3). In February 2016, a relevant episode of Saharan dust outbreak was registered. Two major trends were found: one between 2009 and 2015, at  $4.4\text{--}8.8 \mu\text{g m}^{-3}$ , and another between 2016 and 2017, at  $9.9\text{--}10.1 \mu\text{g m}^{-3}$  (Fig. 4). The increases in this source during the last period are clearly related to fugitive particle emissions from mining activities. The F5 source accounted for 31% of the  $\text{PM}_{10}$  mass, at  $7.7 \mu\text{g m}^{-3}$ .

#### 3.4. Speciation of As in particulate matter during 2015–2017

~~The toxicity of As is dependent on its chemical form, oxidation state, and physical state of gas versus in solution (Pershagen et al., 1982; Viraraghavan et al., 1992).~~ Therefore, a speciation study considering inorganic As species was performed using selected samples of  $\text{PM}_{10}$  from Nerva and La Dehesa containing high As concentrations of more than  $4 \text{ ng m}^{-3}$ . Previous results obtained from 2016 at La Dehesa, located in the vicinity of the Atalaya mine (Fig. 1), prior to implementation of emission abatement technology are included for comparison in Table 2.

To clarify the industrial origin and mining sources of As, the results of inorganic As(III) and As(V) identified by Sánchez-Rodas et al. (2007) and Sánchez de la Campa et al. (2015) were also considered in this study (Table 2). The results show that As(V) was always the main As species at all sampling sites, accounting for >90% of the total As content of the samples. However, the percentages of the extraction differed, at 30% in Cobre las Cruces Mine, 11–12% in this study, and 95% in Huelva. Similar values obtained in La Dehesa, at 12%, and Nerva, at 11%, indicate that the As originated from the same emission source. The low percentage of extraction obtained from Nerva and

La Dehesa rural sites is related to the insoluble nature of the ore extracted in the mine, as a sulphide of Cu–Fe. However, the mean extraction efficiency of the samples obtained from Cobre las Cruces Mine was higher, at about 30%. This difference in extraction efficiency between Nerva and La Dehesa and the Las Cruces mine indicates different mineralogical compositions of the extraction ore of both mines, specifically sulphide of primary origin in pyrite, chalcopyrite, sphalerite, and arsenopyrite in the Atalaya mine and that of secondary origin in covellite in the Las Cruces mine (Sánchez de la Campa et al. (2015). On the contrary, the high extraction percentage in Huelva is related to the oxidation of sulphides in the pyrometallurgy process of the Cu smelter (Sánchez de la Campa et al., 2018; Sánchez-Rodas et al., 2007).

#### 4. Conclusions

Geochemical anomalies in toxic sulphide-associated elements in PM<sub>10</sub> have been identified in the case of the historical Riotinto mine (Iberian Pyrite Belt, Spain) during 2009–2017. In the abandoned mine period (2009–2014), low concentrations of sulphide-associated elements and PM<sub>10</sub> were found (abandoned period: Cu: ng/m<sup>3</sup>, Zn ng/m<sup>3</sup>, Pb ng/m<sup>3</sup> y As ng/m<sup>3</sup>; active mining: Cu ng/m<sup>3</sup> Zn ng/m<sup>3</sup> Pb ng/m<sup>3</sup> y As ng/m<sup>3</sup>). In the periods of reopening and prior to implementation of emission abatement technology, a twofold increase in the concentrations of these elements was observed in 2016, followed by a decrease of 42–59% in 2017.

A seasonal trend was observed for sulphide-associated elements concentrations, with maximum levels occurring mainly in summer associated with sea breezes and North African dust outbreaks, which were more frequent along this period. The minimum concentrations were registered in winter in association with high rainfall and greater frequency of Atlantic front input.

The source contribution analysis using PMF5 has revealed as the mining factor was higher in the reopening period (4.2 µg m<sup>-3</sup>, 16%) compared with the abandoned period (1 µg m<sup>-3</sup>). Finally, the As speciation analysis in the study area indicated that As is mostly present as As(V), at >90% compared with As(III). The low percentage of the extraction obtained during speciation analysis, at 11–12% clearly denotes the association of As and sulphides.

The emission abatement technology of fugitive particles into the atmosphere were effective in order to minimise the impact of APM on the surrounding population. They consist of implementing irrigation, adaptation, and regeneration of tailings and planning of operations using atmospheric dispersion models.

This study has documented as the implementation of the best abatement technologies in historical mines with low ore grade and greater treatment of ore and rock, need a major effort in order to avoid a negative influence on the air quality.

## Acknowledgments

The authors are grateful to various public administrations for financial support: Department of the Environment (project 10/2013/PC/00) and Department of Innovation, Science and Enterprise (project 2009-RNM 5163M and 2011 RNM 7800) of the Autonomous Government of Andalusia and Project CGL2008-06270-C02/CLI of the Spanish Educational Ministry. In addition, the environmental technicians at Atalaya Mining and Nerva Town Hall are thanked for providing assistance with the sampling.

## References

Alastuey, A., Querol, X., Plana, F., Viana, M., Ruiz, C.R., Sánchez de la Campa, A., de la Rosa, J., Mantilla, E., García dos Santos, S., 2006. Identification and Chemical Characterization of Industrial Particulate Matter Sources in Southwest Spain. *J. Air Waste Manag. Assoc.* 56, 993-1006.

Bell, F.G., Bullock, S.E.T., Haibich, T.F.J., Lindsay, P., 2001. Environmental impacts associated with an abandoned mine in the Witbank Coalfield, South Africa. *Int. J. Coal Geol.* 45, 195–216.

Brotos, J.M., Romero Diaz, A., Sarria, F.A., Serrato, F.B., 2010. Wind erosion on mining waste in southeast Spain. *Land Degrad Dev*; 21, 196–209.

Carslaw, D.D., Ropkins, K., 2012a. Openair-an R package for air quality data analysis. *Environ. Model Software* (27-28) 52-61.

Carslaw, D.D., Ropkins, K., 2012b. Openair: Open-source Tools for the Analysis of Air Pollution Data (Computer Program) (European) <http://www.openair-project.org>. (Accessed 9 January 2018).

Castillo, S., De la Rosa, J.D., Sánchez de la Campa, A.M., González-Castanedo, Y., Fernández-Caliani, J.C., González, I., Romero, A., 2013. Contribution of mine wastes to atmospheric metal deposition in the surrounding area of an abandoned heavily polluted mining district (Rio Tinto mines, Spain). *Sci. Total Environ.* 449, 363–372.

CEMI (The Centre for Excellence in Mining Innovation) 2010. Literature Review of Current Fugitive Dust Control Practices within the Mining Industry, pp 49. (web link <https://www.cemi.ca/wp-content/uploads/2017/06/Literature.pdf> )

Csavina, J., Landázuri, A., Wonaschütz, A., Rine, K., Rheinheimer, P., Barbaris, B., Conant, W., Sáez, A.E., Betterton, E.A., 2011. Metal and metalloid contaminants in atmospheric aerosols from mining operations. *Water Air Soil Pollut.* 221, 145–157.

Csavina, J., Field, J., Taylor, M.P., Gao, S., Landázuri, A., Betterton, E.A., Eduardo, A., 2012. A review on the importance of metals and metalloids in atmospheric dust and aerosol from mining operations. *Sci. Total Environ.* 433, 58–73.

Davis, R.A. Jr., Welty, A.T., Borrego, J., Morales, J.A., Pendon, G., Ryan, J.G., 2000. Rio Tinto estuary (Spain): 5000 years of pollution. *Environ. Geol.* 39, 1107–1116.

Galán, E., Gómez-Ariza, J.L., González, I., Fernández-Caliani, J.C., Morales, E., Giraldez, I., 2003. Heavy metal partitioning in river sediments severely polluted by acid mine drainage in the Iberian Pyrite Belt. *Appl. Geochem.* 18, 409–421.

Leistel, J.M., Marcoux, E., Thiéblemont, D., Quesada, C., Sánchez, A., Almodóvar, G.R., Pascual, E., Sáez, R., 1998. The volcanic-hosted massive sulphide deposits of the Iberian Pyrite Belt. *Miner. Depos.* 33, 2–30.

Lottermoser, B.G., 2010. *Mine Wastes, Characterization, Treatment, Environmental Impacts* 3rd Edition. Springer-Verlag, Berlin.

Magas, O.K., Gunter, J.T., Regens, J.L., 2007. Ambient air pollution and daily pediatric hospitalizations for asthma. *Environ. Sci. Pollut. Res.* 14, 19–23.

Nriagu, J.O., Pacyna, J.M., 1988. Quantitative assesment of worldwide contamination of air, water and soils by trace metals. *Nature* 333, 134-139.

Oliveira, V., Gómez-Ariza, J.L., Sánchez-Rodas, D., 2005. Extraction procedures for chemical speciation of arsenic in atmospheric total suspended particles. *Anal. Bioanal. Chem.* 382, 335–340.

Park, S.S., Kim, Y.J., 2005. Source contributions to fine particulate matter in an urban atmosphere. *Chemos.* 59, 217–226.

Patra, A.K., Gautam, S., Kumar, P., 2016. Emissions and human health impact of particulate matter from surface mining operation—A review. *Env. Tech. & Innov.* 5, 233-249.

Pershagen, G., Lind, B., Bjorklund, N.E., 1982. Lung retention and toxicity of some inorganic arsenic compound. *Environ. Res.* 29, 425–434.

Plumlee, G.S., Morman, S.A., 2011. Mine wastes and human health. *Elements*, 7, 399–404.

Querol, X., Alastuey, A., Rodríguez, S., Plana, F., Ruiz, C.R., Cots, N., Massagué, G., Puig, O., 2001. PM<sub>10</sub> and PM<sub>2.5</sub> source apportionment in the Barcelona Metropolitan Area, Catalonia Spain. *Atmos. Environ.* 35, 6407–6419.

Querol, X., Alastuey, A., de la Rosa, J., Sánchez de la Campa, A., Plana, F., Ruiz, C.R., 2002. Source apportionment analysis of atmospheric particles in an industrialised site in southwestern Spain. *Atmos. Environ.* 36, 2113–3125.

Querol, X., Alastuey, A., Ruiz, C.R., Artiñanob, B., Hansson, H.C., Harrison, R.M., Buringh, E., ten Brink, H.M., Lutzg, M., Bruckmann P., Straehl, P., Schneider, J., 2004. Speciation and origin of PM<sub>10</sub> and PM<sub>2.5</sub> in selected European cities. *Atmos. Environ.* 38, 6547–6555.

Querol, X., Alastuey, A., Moreno, T., Viana, M.M., Castillo, S., Pey, J., Rodríguez, S., Artiñano, B., Salvador, P., Sánchez, M., Garcia Dos Santos, S., Herce Garraleta, M.D., Fernandez-Patier, R., Moreno-Grau, S., Negral, L., Minguillón, M.C., Monforte, E., Sanz, M.J., Palomo-Marín, R., Pinilla-Gil, E., Cuevas, E., de la Rosa, J., Sánchez de la Campa, A., 2008. Spatial and temporal variations in airborne particulate matter (PM<sub>10</sub> and PM<sub>2.5</sub>) across Spain 1999–2005. *Atmos. Environ.* 42, 3964–3979.

Rasmussen, P.E., 1998. Long-range atmospheric trans- port of trace metals: the need for geoscience perspectives, *Environ. Geol.* 33, 96–108.

Rodríguez, S., Querol, X., Alastuey, A., Kallos, G., Kakaliagou, O., 2001. Saharan dust contributions to PM<sub>10</sub> and TSP levels in Southern and Eastern Spain. *Atmos. Environ.* 35, 2433–2447.

Sánchez de la Campa, A.M., Sánchez-Rodas, D., González-Castanedo, Y., de la Rosa, J.D., 2015. Geochemical anomalies of toxic elements and arsenic speciation in airborne particles from Cu mining and smelting activities: influence on air quality. *J. Haz. Mat.* 291, 18–27.

Sánchez de la Campa, A.M., de la Rosa, J.D., Fernández-Caliani, J.C, González-Castanedo, Y., 2011. Impact of abandoned mine wastes on atmospheric respirable particulate matter in the historic mining district of Rio Tinto (Iberian Pyrite Belt). *Environ. Res.* 111, 1018–1023.

Sánchez de la Campa, A.M., de la Rosa, J.D., Sánchez-Rodas, D., Oliveira, V., Alastuey, A., Querol, X., Gómez-Ariza, J.L., 2008. Arsenic speciation study of PM<sub>2.5</sub> in an urban area near a copper smelter. *Atmos. Environ.* 42, 6487–6495.

Sánchez de la Campa, A.M., Sánchez-Rodas, D., Alsioufi, L., Alastuey, A., Querol, X., de la Rosa, J.D., 2018. Air quality trends in an industrialised area of SW Spain. *J. Clean. Prod.* 186, 465–474.

Sánchez-Rodas, D., Sánchez de la Campa, A.M., de la Rosa, J.D., Oliveira, V., Gómez Ariza, J.L., Querol, X., Alastuey, A., 2007. Arsenic speciation of atmospheric particulate matter (PM<sub>10</sub>) in an industrialised urban site in southwestern Spain. *Chemos.* 66, 1485–1493.

Singh, G., Sharma, P.K., 1992. A study of spatial-distribution of air- pollutants in some coal-mining areas of Raniganj coalfield, India. *Environ. Inter.* 18, 191–200.

Taylor, M.P., Mackay, A.K., Hudson-Edwards, K.A., Holz, E., 2010. Soil Cd, Cu, Pb and Zn contaminants around Mount Isa city, Queensland, Australia: potential sources and risks to human health. *Appl. Geochem.* 25, 841–55.

Tsai, Y.I., Cheng, M.T., 2004. Characterization of chemical species in atmospheric aerosols in a metropolitan basin, *Chemos.* 54, 1171–1181.

Viana, M., Kuhlbusch, T.A.J., Querol, X., Alastuey, A., Harrison, R.M., Hopke, P.K., Winiwarter, W., Vallius, M., Szidat, S., Prévôt, A.S.H., Hueglin, C., Bloemen, H., Wählin, P., Vecchi, R., Miranda, A.I., Kasper-Giebl, A., Maenhaut, W., Hitenberger, R., 2008. Source apportionment of particulate matter in Europe: A review of methods and results. *J. Aero. Sci.* 239, 827–849.

Viana, M., Hammingh, P., Colette, A., Querol, X., Degraeuwe, B., de Vlieger, I., van Aardenne, J.I., 2014. Impact of maritime transport emissions on coastal air quality in Europe, *Atmos. Environ.* 90, 96–105.

Viraraghavan, T., Jin, Y.C., Tonita, P.M., 1992. Arsenic in water supplies. *Int. J. Environ. Stud.* 41, 159–167.

Wai, K., Wu, S., Li, X., Jaffe, D.A., Perry, K.D., 2016. Global atmospheric transport and source-receptor relationships for arsenic. *Environ. Sci. Technol.* 50, 3714–3720.

Wild, P., Bourgard, E., Paris, C., 2009. Lung cancer and exposure to metals: the epidemiological evidence. *Method. Molecular Biology.* 472, 139–167.

WHO (World Health Organization), 2013. Review of Evidence on Health Aspects of Air Pollution-REVIHAAP Project. Technical report. [http://www.euro.who.int/\\_data/assets/pdf\\_file/0004/193108/REVIHAAP-Final-technical-report.pdf](http://www.euro.who.int/_data/assets/pdf_file/0004/193108/REVIHAAP-Final-technical-report.pdf) . (Accessed 23 January 2020).

Zota, A.R., Willis, R., Rebecca, J., Norris, G.A., Shine, J.P., 2009. Impact of mine waste on airborne respirable particulates in Northeastern Oklahoma, United States. *J. Air Waste Manage. Assoc.* 59, 1347–1357.

Figure captions

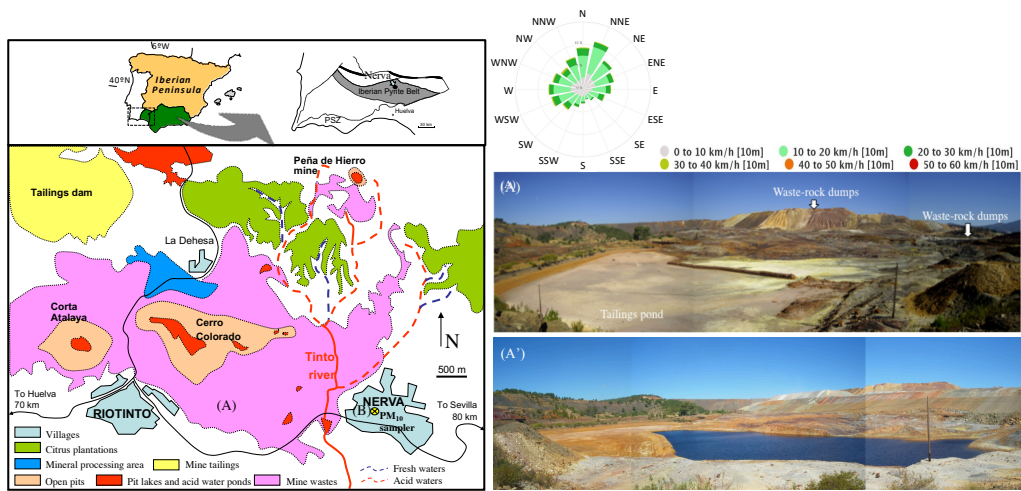


**Fig. 1.** Map of the Riotinto Mining District and location of the PM<sub>10</sub> sampler in Nerva. (A–A') Panoramic view of the Riotinto mining area showing tailings and waste-rock dumps prior to and during the mine reopening.

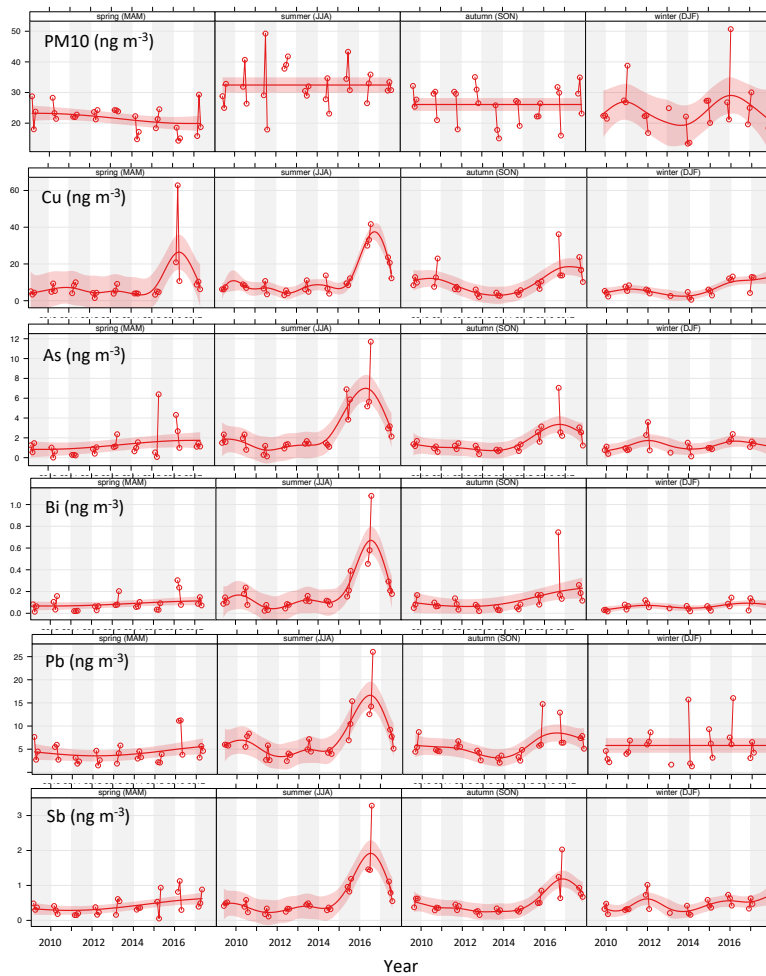


**Fig. 2.** Seasonal variation of PM<sub>10</sub> and sulphide-associated elements (Cu, As, Bi, Pb and Sb) for the period 2009–2017. Dots correspond to monthly mean concentrations. The solid lines and bands stand for the smooth trend with a 95% confidence interval. Spring (MAM): March, April, May; Summer (JJA): June, July, August; Autumn (SON): September, October, November.

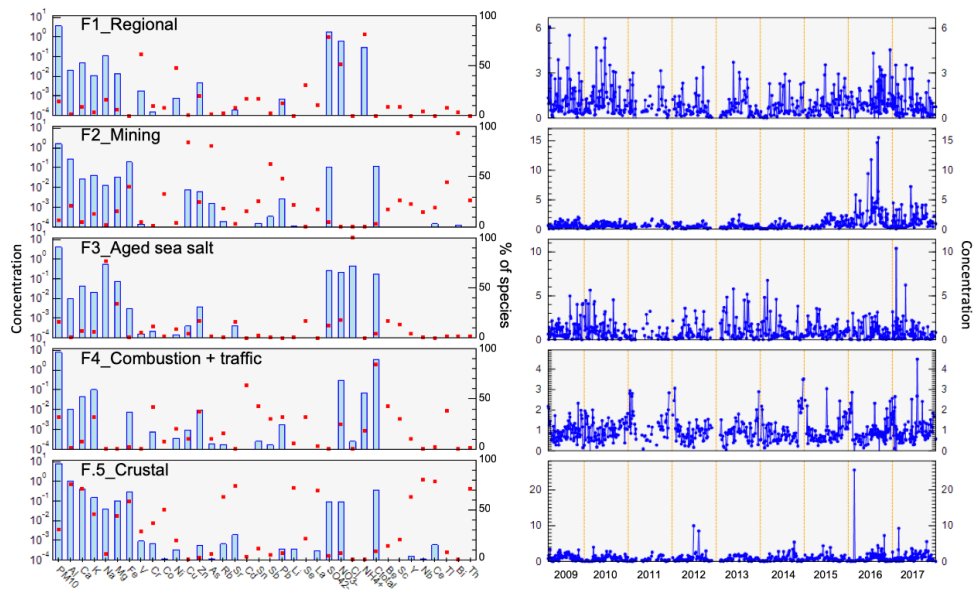


**Fig. 3.** Source profiles (left panels) and temporal evolutions (right panels) of contributions of primary factors.

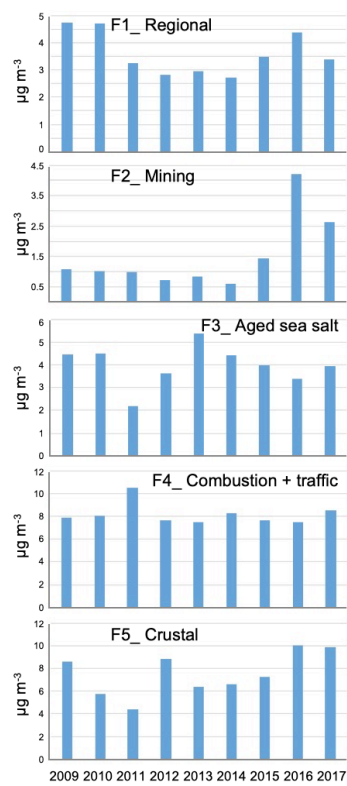


**Fig. 4.** Source contribution registered in each year at Nerva station.

**Table 1.**

Mean concentrations of PM ( $\mu\text{g m}^{-3}$ ) and sulphide-associated elements ( $\text{ng m}^{-3}$ ) in PM<sub>10</sub>, showing differences in three periods of mine abandonment and during and after emission abatement technology implementation at the Cu mine in 2009–2017. The trend estimate and statistical significance are  $p < 0.001 = \text{***}$ ,  $p < 0.01 = \text{**}$ ,  $p < 0.05 = \text{*}$ , and  $p < 0.1 = \text{+}$ .

Sampling period	Abandonment mine		During		After 2017	Trend estimate ( $\mu\text{g m}^{-3} \cdot \text{year}^{-1}$ )	Statistical Significance
	2009-2014		2015	2016			
$\mu\text{g m}^{-3}$	mean		mean	mean	mean		
n° filters	348		59	80	80		
PM <sub>10</sub>	26		27	27	27	-0,15	
C <sub>total</sub>	4,12		3,67	4,27	4,60	0,1	
C org*	3,82		2,15	3,85	4,28		
Cnm*	3,92		1,93	0,43	0,40		
CO <sub>3</sub> <sup>=</sup>	1,32		1,56	1,96	1,68	0,04	
SiO <sub>2</sub>	3,19		4,56	6,41	5,55	0,26	**
Al <sub>2</sub> O <sub>3</sub>	1,06		1,51	2,14	1,85	0,09	**
Ca	0,56		0,64	0,79	0,66	0,01	
K	0,31		0,33	0,45	0,46	0,02	***
Na	0,75		0,69	0,66	0,71	-0,01	
Mg	0,19		0,24	0,31	0,27	0,01	*
Fe	0,37		0,44	0,88	0,74	0,03	***
PO <sub>4</sub> <sup>3-</sup>	0,06		0,06	0,09	0,14	0,01	***
SO <sub>4</sub> <sup>2-</sup>	2,21		2,09	2,92	2,32	0,02	
SO <sub>4</sub> <sup>2-</sup> anthrop.	2,02		1,92	2,76	2,14	0,02	
SO <sub>4</sub> <sup>2-</sup> marine	0,19		0,17	0,17	0,18	0	
NO <sub>3</sub> <sup>-</sup>	1,34		1,34	2,74	1,39	0	
Cl	0,56		0,50	0,48	0,52	0	
NH <sub>4</sub> <sup>+</sup>	0,47		0,43	0,48	0,37	-0,01	*
$\text{ng/m}^3$							
Li	0,40		0,47	0,76	0,69	0,04	***
Be	0,01		0,02	0,03	0,03	0	***
Sc	0,09		0,12	0,21	0,22	0,01	***
Ti	35,6		48,4	62,4	54,1	1,87	*
V	2,78		2,85	3,82	3,14	0,06	
Cr	1,83		2,42	2,53	2,03	0,11	*
Mn	8,66		70,0	14,1	14,7	0,71	**
Co	0,19		0,19	0,36	0,32	0,01	**
Ni	1,81		1,32	1,79	3,44	0,04	
Cu	6,10		7,65	25,3	14,8	0,69	**
Zn	23,2		21,7	49,1	21,1	0,34	
Ga	0,47		0,17	0,35	0,30	-0,02	*
Ge	0,05		0,03	0,06	0,16	0	*
As	1,12		2,98	4,47	1,97	0,13	***
Se	0,34		0,22	0,13	0,13	-0,01	*
Rb	0,95		0,99	1,53	1,33	0,04	*
Sr	2,27		2,39	3,33	2,82	0,08	+
Y	0,20		0,19	0,41	0,40	0,02	***
Zr	1,56		2,11	4,19	7,44	0,31	***
Nb	0,11		0,10	0,20	0,22	0,01	*
Mo	3,27		4,83	5,54	5,80	0,34	**
Cd	0,14		0,13	0,15	0,23	0	
Sn	0,59		0,60	0,78	0,63	0	
Sb	0,36		0,67	1,31	0,70	0,05	***
Cs	0,05		0,05	0,09	0,08	0	**
Ba	13,0		11,9	24,1	12,4	0,33	
La	0,35		0,37	0,65	0,52	0,02	*
Ce	0,62		0,66	1,19	1,02	0,04	*
Lu	0,01		0,01	0,01	0,01	0	
Hf	0,07		0,08	0,19	0,29	0,01	***
Ta	0,01		0,01	0,01	0,02	0	
W	0,03		0,07	0,04	0,11	0	
Tl	0,03		0,03	0,06	0,03	0	***
Pb	4,75		7,20	11,5	6,12	0,22	*
Bi	0,08		0,13	0,39	0,16	0,01	***
Th	0,09		0,10	0,17	0,17	0,01	***
U	0,04		0,04	0,08	0,08	0	**

C org\* and Cnm\* in NERVA 2014, 2015, 2016 and 2017 are replaced by the OC and EC analyses.

**Table 2.**

Total As concentration, As species, and percentage of As extraction in PM<sub>10</sub> samples collected in 2016 from Nerva and La Dehesa. Data of Huelva, Gerena, and Cobre las Cruces Mine are included for comparison. The results expressed as ng m<sup>-3</sup> (mean ± standard deviation). N indicates the number of samples.

Sampling site	N	As <sub>total</sub> <sup>a</sup>	As(III) <sup>b</sup>	As(V) <sup>b</sup>	% Extraction	Reference
Huelva	22	16.4 ± 11.7	0.4 ± 0.3	14.9 ± 13.1	94 ± 19	Sánchez Rodas et al. (2007)
Cobre las Cruces Mine	23	36.2 ± 25.6	0.3 ± 4.3	8.5 ± 4.3	30 ± 15	Sánchez de la Campa et al. (2015)
La Dehesa	5	25.3 ± 10.7	0.3 ± 0.1	2.5 ± 1.1	12 ± 4.5	This study
Nerva	1	43.4	0.4	4.2	11	

<sup>a</sup> As<sub>total</sub> calculated after acid digestion and determination by ICP-MS.

<sup>b</sup> As(III) and As(V) calculated after liquid extraction and determination by HPLC-HG-AFS.

## SUPPLEMENTARY DATA

**Article title:**  
**2009-2017 TRENDS OF AIR QUALITY IN THE LEGENDARY RIOTINTO MINING  
DISTRICT OF SW SPAIN**

Ana M. Sánchez de la Campa<sup>a,b\*</sup>, Daniel Sánchez-Rodas<sup>a,c</sup>, Gonzalo Márquez<sup>a,b</sup>, Emilio Romero<sup>b</sup>, Jesús D. de la Rosa<sup>a,d</sup>

<sup>a</sup> Center for Research in Sustainable Chemistry-CIQSO, Associate Unit CSIC-University of Huelva “Atmospheric Pollution”, Campus El Carmen s/n, 21071 Huelva, Spain

<sup>b</sup> Department of Mining, Mechanic, Energetic and Construction Engineering, ETSI, University of Huelva, 21071 Huelva, Spain

<sup>c</sup> Department of Chemistry, Faculty of Experimental Sciences, University of Huelva, 21071 Huelva, Spain

<sup>d</sup> Department of Department of Earth Sciences, Faculty of Experimental Sciences, University of Huelva, 21071 Huelva, Spain

\*Presenting author email: [ana.sanchez@pi.uhu.es](mailto:ana.sanchez@pi.uhu.es)

**Table S1.** Case studies according to mineral exploitation, transport, abandoned mine, mining waste accidents and bioaccessibility and health risk, related to air quality and coal, metallic and no-metallic ore mining.

	<b>Coal</b>	<b>Metallic ore</b>	<b>no metallic ore</b>
<b>Exploitation</b>	India (Ghose and Majee, 2000) Wales (Jones et al., 2002) India (Chaulya 2004., 2005) Turkey (Onder and Yigit., 2009) Colombia (Huertas et al., 2012a; 2012b) Australia (Richardson et al., 2019)	Ni-Cu, Bostwana (Ekosse., 2004) Cu, Marocco (El Khalil et al., 2008) Sb, China (Zhang et al., 2008) Cu, Mexico (Meza-Figueroa et al., 2009) As, China (Zhao et al., 2019) Au-Ag-Pb-Zn-Cu, Australia (Schneider et al. 2019)	Hg-Sb, China (Ao et al. 2019., 2020) Diamand, Canada (Liberda et al., 2015) Limestone, China (Peng et al., 2016)
<b>Transport</b>	Appalachia, USA (Aneja et al., 2012)	Fe, India (Sinha et al., 1997) Au, Nevada, USA (McDonald et al., 2003) Fe, Australia (Hinwood et al., 2014) Au, Canada (Wong et al., 1999) Pb-Cu-Zn, Germany (Kempter and Frenzel., 2000) Au, Spain (Moreno et al., 2007) Pb-Zn, Oklaoma (Zota et al., 2009) Cu, Spain (Sánchez de la Campa et al., 2011) Ag-Sn, Bolivia (Fontúrbel et al., 2011) Fe-Cu-Pb-Zn-Ag, Italy (Comero et al., 2012) Au, Australia (Martín et al., 2017) Pb-Zn-Fe, Spain (Sánchez Bisquert et al., 2017) Pollimetalic, Spain (Blondet et al., 2019)	---
<b>Abandonment of mining</b>	S Africa (Bell et al., 2001)		Hg, Spain (Moreno et al., 2005) Hg, Spain (Loredo et al., 2007)
<b>Mining waste accidents</b>	---	Cu, Spain (Querol et al., 1999, 2000)	---
<b>Bioaccessibility and Health risk</b>	England, Pless-Mullooli et al., (2000) China (Jia., 2015)	Cu, Korea (Kim et al., 2008) Ni, China (Li and Hu., 2018) Pb-Zn-Mn, China (Du et al., 2019) Pb-Cu-Zn-Ag-V, Namibia (Ettler et al., 2019) U, France (Husson et al., 2019) REE, China (Tian et al., 2019)	---

1 **References**

- 2 Aneja, V.P., Isherwood, A., Morgan, P., 2012. Characterization of particulate matter  
3 (PM10) related to surface coal mining operations in Appalachia. *Atmos. Environ.* 54,  
4 496–501.
- 5
- 6 Bell, F.G., Bullock, S.E.T., Hälbich, T.F.J., Lindsay, P., 2001. Environmental impacts  
7 associated with an abandoned mine in the Witbank Coalfield, South Africa. *Inter. Journal*  
8 *Coal Geo.* 45, 195–216.
- 9
- 10 Blondet, I., Schreck, E., Viers, J., Casas, S., Jubany, I., Bahí, N., Zouiten, C., Dufréhou,  
11 G., Freydier, R., Galy-Lacaux, C., Martínez-Martínez, S., Faz, A., Soriano-Disla, M.,  
12 Acosta, J.A., Darrozes, J., 2019. Atmospheric dust characterisation in the mining district  
13 of Cartagena-La Unión, Spain: Air quality and health risks assessment. *Sci. Total*  
14 *Environ.* 693, 133496.
- 15
- 16 Chaulya, S.K., 2004. Assessment and management of air quality for an opencast coal  
17 mining area. *J. Environ. Manage.* 70, 1–14.
- 18
- 19 Chaulya, S.K., 2005. Air quality status of an open pit mining area in India. *Environ. Monit.*  
20 *Assess.* 105, 369–389.
- 21
- 22 Comero, S., Servida, D., De Capitani, L., Manfred Gawlik, B., 2012. Geochemical  
23 characterization of an abandoned mine site: A combined positive matrix factorization and  
24 GIS approach compared with principal component analysis. *J. Geo. Exp.* 118, 30–37.
- 25
- 26 Du, Y., Chen, L., Ding, P., Liu, L., He, O., Chen, B., Duan, Y., 2019. Different exposure  
27 profile of heavy metal and health risk between residents near a Pb-Zn mine and a Mn  
28 mine in Huayuan county, South China. *Chemos.* 216, 352–364
- 29
- 30 Ekosse, G., Van den Heever, D.J., de Jager, L., Totolo, O., 2004. Environmental  
31 chemistry and mineralogy of particulate air matter around Selebi Phikwe nickel–copper  
32 plant, Botswana. *Minerals Engineering* 17, 349–353.
- 33
- 34 El Khalil, H., El Hamiani, O., Birron, G., Ouazzani, N., Boularbah, A., 2008. Heavy metal  
35 contamination from mining sites in South Morocco: Monitoring metal content and toxicity  
36 of soil runoff and groundwater. *Environm. Monit. Asses.* 136, 147–160.
- 37
- 38 Fontúrbel, F.E., Barbieri, E., Herbas, C., Barbieri, F.L., Gardon, J., 2011. Indoor metallic  
39 pollution related to mining activity in the Bolivian Altiplano. *Environ. Poll.* 159, 2870–  
40 2875.
- 41
- 42 Ghose, M.K., Majee, S.R., 2000. Assessment of the impact on the air environment due  
43 to opencast coal mining – and Indian case study. *Atmos. Environ.* 34, 2791-2796.
- 44

45 Hinwood, A., Callan, A.C., Heyworth, J., McCafferty, P., Sly, P.D., 2014. Children's  
46 personal exposure to PM10 and associated metals in urban, rural and mining activity  
47 areas. *Chemos.* 108,125–133.

48

49 Huertas, J.I., Huertas, M.E., Solís, D.A., 2012a. Characterization of airborne particles in  
50 an open pit mining región. *Sci. Total Environ.* 423, 39–46.

51

52 Huertas J.I, Huertas M.E, Izquierdo S, González E.D (2012b). Air quality impact  
53 assessment of multiple open pit coal mines in northern Colombia. *Journal of*  
54 *Environmental Management* 93 (2012) 121-129.

55

56 Husson, A., Leermakers, M., Descostes, M., Lagneau, V., 2019. Environmental  
57 geochemistry and bioaccumulation/bioavailability of uranium in a post-mining context e  
58 The Bois-Noirs Limouzat mine (France). *Chemos.* 236, 124341.

59

60 Jia, J., Li, X., Wu, P., Liu, Y., Han, C., Zhou, L., Yang, L., 2015. Human Health Risk  
61 Assessment and Safety Threshold of Harmful Trace Elements in the Soil Environment  
62 of the Wulantuga Open-Cast Coal Mine. *Minerals* 2015, 5, 837–848.

63

64 Jones, T., Blackmore, P., Leach, M., Bérubé, K., Sexton, K., Richards, R., 2002.  
65 Characterisation of airborne particles collected within and proximal to an opencast  
66 coalmine: South Wales, U.K. *Environ. Monit. and Assess.* 75, 293–312.

67

68 Kempter, H., Frenzel, B., 2000. The impact of early mining and smelting on the local  
69 tropospheric aerosol detected in ombrotrophic peat bogs in the Harz, Germany. *Water,*  
70 *Air, and Soil Poll.* 121, 93–108.

71

72 Kim, S., Kwon, H., Cheong, H., Choi, K., Jang, J., Jeong, W., Kim, D., Lee, K., Yang, S.,  
73 Jhung, I., Yang, W., Hong, Y., 2008. Investigation on Health Effects of an Abandoned  
74 Metal Mine. *J. Korean Med. Sci.* 23, 452-8.

75

76 Li, Z., Hu, B., 2018. Perceived health risk, environmental knowledge, and contingent  
77 valuation for improving air quality: New evidence from the Jinchuan mining area in China.  
78 *Econ. Hum. Biol.* 31, 54–68

79

80 Loredo, J., Soto, J., Álvarez, R., Ordóñez, A., 2007. Atmospheric Monitoring at  
81 Abandoned Mercury Mine Sites in Asturias (NW Spain). *Environ. Monit. Assess.* 130,  
82 201–214.

83

84 Martin, R., Dowling, K., Pearce, D.C, Florentine, S., McKnight, S., Stelcer, E., Cohen,  
85 D.D., Stopic, A., Bennett, J.W., 2017. Trace metal content in inhalable particulate matter  
86 (PM<sub>2.5-10</sub> and PM<sub>2.5</sub>) collected from historical mine waste deposits using a laboratory-  
87 based approach. *Environ. Geochem. Health* 39, 549–563.

88

89 McDonald, J.D., Zielinska, B., Sagebiel, J.C., McDaniel, M.R., Mousset, J.P., 2003.  
90 Source apportionment of airborne fine particulate matter in an underground mine. *J. Air*  
91 *Waste Manag. Assoc.* 53, 386–395.

92

93 Meza-Figueroa, D.M., Maier, R.M., de la O-Villanueva M., Gómez-Alvarez, A., Moreno-  
94 Zazueta, A., Rivera, J., Campillo, A., Grandlic, C.J., Anaya, R., Palafox-Reyes, J., 2009.  
95 The impact of unconfined mine tailings in residential areas from a mining town in a semi-  
96 arid environment: Nacozari, Sonora, Mexico. *Chemos.* 77, 140–147.

97

98 Moreno, T., Higuera, P., Jones, T., McDonald, I., Gibbons, W., 2005. Size fractionation  
99 in mercury-bearing airborne particles (HgPM<sub>10</sub>) at Almadén, Spain: Implications for  
100 inhalation hazards around old mines. *Atmos. Environ.* 39, 6409–6419.

101

102 Moreno, T., Oldroyd, A., McDonald, I., Gibbons, W., 2007. Preferential Fractionation of  
103 Trace Metals–Metalloids into PM<sub>10</sub> Resuspended from Contaminated Gold Mine  
104 Tailings at Rodalquilar, Spain. *Water Air Soil. Pollut.* 179, 93–105.

105

106 Onder, M., Yigit, E., 2009. Assessment of respirable dust exposures in an opencast coal  
107 mine. *Environ. Monit. Assess.* 152, 393–401.

108

109 Pless-Mulloli, T., King, A., Howel, D., Stone, I., Merefield, J., 2000. PM<sub>10</sub> levels in  
110 communities close to and away from opencast coal mining sites in northeast England.  
111 *Atmos. Environ.* 34, 3091–3101.

112

113 Querol, X., Alastuey, A., López-Soler, A., Plana, F., Mesas, A., Ortiz, L., Alzaga, R.,  
114 Bayona, J.M., de la Rosa, J., 1999. Physico-chemical characterisation of atmospheric  
115 aerosols in a rural area affected by the aznalcollar toxic spill, south-west Spain during  
116 the soil reclamation activities. *Sci. Total Environ.* 242, 89–104.

117

118 Querol, X., Alastuey, A., López-Soler, A., Plana, F., 2000. Levels and chemistry of  
119 atmospheric particulates induced by a spill of heavy metal mining wastes in the Doñana  
120 area, Southwest Spain. *Atmos. Environ.* 34, 239–253.

121

122 Richardson, C., Rutherford, S., Agranovski, I.E., 2019. Open cut black coal mining:  
123 Empirical verification of PM<sub>2.5</sub> air emission estimation techniques. *Atmos. Res.* 216,  
124 151–159.

125

126 Sánchez de la Campa, A.M., de la Rosa, J.D., Fernández Caliani, J.C, Gonzalez-  
127 Castanedo, Y., 2011. Impact of abandoned mine wastes on atmospheric respirable  
128 particulate matter in the historic mining district of Rio Tinto (Iberian Pyrite Belt). *Environ.*  
129 *Res.* 111, 1018-1023.

130 Sánchez Bisquert, D., Peñas Castejón, J. M., García Fernández, G., 2017. The impact  
131 of atmospheric dust deposition and trace elements levels on the villages surrounding the  
132 former mining areas in a semi-arid environment (SE Spain) *Atmos. Environ.* 152, 256–  
133 269.

134

135 Schneider, L., Mariani, M., Saunders, K.M., Maher, W.A., Harrison, J.J., Fletcher, M.S.,  
136 Zawadzki, A., Heijnis, H., Haberle S.G., 2019. How significant is atmospheric metal  
137 contamination from mining activity adjacent to the Tasmanian Wilderness World Heritage  
138 Area? A spatial analysis of metal concentrations using air trajectories models. *Sci. Total*  
139 *Environ.* 656, 250–260.

140

141 Sinha, S., Banerjee, S.P., 1997. Characterization of haul road dust in an Indian opencast  
142 iron ore mine. *Atmos. Environ.* 17, 2809–2814.

143

144 Tian, S., Liang, T., Li, K., 2019. Fine road dust contamination in a mining area presents  
145 a likely air pollution hotspot and threat to human health. *Environ. Inter.* 128, 201–209.

146

147 Ettler, V., Cihlová, M., Jarošíková, A., Mihaljevič, M., Drahot, P., Kříbek, B., Vaněk, A.,  
148 Penížek, V., Sracek, O., Klementová, M., Engel, Z., Kamona, F., Mapani, B., 2019. Oral  
149 bioaccessibility of metal(loid)s in dust materials from mining areas of northern Namibia.  
150 *Environ. Inter.* 124, 205–215.

151

152 Wong, H.K.T., Gauthier, A., Nriagu, J.O., 1999. Dispersion and toxicity of metals from  
153 abandoned gold mine tailings at Goldenville, Nova Scotia, Canada. *Sci. Total Environ.*  
154 228, 35–47.

155

156 Zhao, C., Yang, J., Zheng, Y., Yang, J., Guo, G., Wang, J., Chen, T., 2019. Effects of  
157 environmental governance in mining areas: The trend of arsenic concentration in the  
158 environmental media of a typical mining area in 25 years. *Chemos.* 235, 849–857.

159

160 Zhang, X., Tang, X., Zhao, C., Zhang, G., Hu, H., Wu, H., Hu, B., Mo, L., Huang, L., Wei,  
161 J., 2008. Health Risk Evaluation for the Inhabitants of a Typical Mining Town in a  
162 Mountain Area, South China. *Ann. N.Y. Acad. Sci.* 1140, 263–273.

163

164 Zota, A.R., Willis, R., Rebecca, J., Norris, G.A., Shine, J.P., 2009. Impact of Mine Waste  
165 on Airborne Respirable Particulates in Northeastern Oklahoma, United States. *J. Air*  
166 *Waste Manage. Assoc.* 59, 1347–1357.

167

168

169

170

171

172